

Achromatic Total Internal Reflection Prism in DLP Projection System

Ya-Chi Lu¹, Jhong-Syuan Li², Kao-Der Chang³, Shie-Chang Jeng⁴
Jui-Wen Pan²

¹ Institute of Lighting and Energy Photonics, National Chiao Tung University, Taiwan,

² Institute of Photonic System, National Chiao Tung University, Taiwan

³ Mechanical and Mechatronics Systems Research Laboratories, Industrial Technology Research Institute, Taiwan

⁴ Institute of Imaging and Biomedical Photonics, National Chiao Tung University, Taiwan

Keywords: DLP Projection System, Large Area Displays, Total Internal Reflection Prism

ABSTRACT

Two different types of the achromatic TIR prism set are designed to mini projector. Type1 prism set is the first prism with a small Abbe number material stacked with the second prism with a large Abbe number material. Type2 prism set is an opposite design to Type1 prism set.

1. INTRODUCTION

Nowadays, solid-state light sources, such as LED and Laser, are widely utilized as a light source of a projection system. As a solid-state light source is applied, an additional component to generate RGB light is no more needed. This is a great difference between the traditional light source and solid-state light source. For a color display, three Lasers respectively with red, green, and blue wavelengths are necessary [1]. Compared to the laser, LED as light source has some advantages [2–9]. Therefore, in this paper, the LEDs is chosen as our light source for the projection system. However, there is chromatic uniformity issue such as the lateral color aberration at the corner of the projection screen. In order to solve this issue, an achromatic design is necessary. In order to reduce color aberration without extra lenses, an achromatic total internal reflection (ATIR) prism set is proposed.

2. RESULTS

2.1 Definitions of achromatic TIR prism

The schematic of ATIR prism is shown in Fig.1. ATIR prism set consists of the first prism, the second prism stacking with a Digital micromirror device (DMD), DLP® 0.3 WVGA DMD [10]. The first prism has an apex angle of θ_1 as shown in Fig.1. The second prism is an isosceles right-angled triangle. The refraction index of the first prism and the second prism is denoted by n_1 and n_2 , respectively. The optical axis ray passes through the ATIR prism set and impinges on DMD chip with an angle of θ_{DMD} . θ_{in} is the incident angle of optical axis ray at the first prism and θ_{DMD} is the incident angle at the DMD active area. The angle of θ_{in} is positive while the optical axis ray is rotated clockwise to reach the normal of the entrance of the first

prism. Moreover, the prism size decreases when θ_{in} increases due to the relation among prism size, θ_{in} and θ_1 .

The ATIR prism is designed to reduce the lateral color aberration. We choose appropriate prism combinations to eliminate the lateral chromatic aberration. V_1 and V_2 represent the Abbe number of the first prism and the second prism, respectively. The difference of Abbe number is responsible to eliminate the lateral color aberration of the ATIR prism set [11]. As mentioned before, type1 prism set consists of a small Abbe number prism stacked with a high Abbe number one. In order to optimized the achromatic capability of the ATIR prism set, five optical materials with Abbe number lower than 50 are considered. The five optical materials are N-SSK8, N-BAF10, N-LAF2, N-SF2 and N-SF57 [12]. The material of the second prism is N-BK7. For type2 prism set, the material of the first prism is assumed to be N-BK7. The considered small Abbe number materials for the second prism are N-SSK8, N-BAF10, N-LAF2, N-SF2 and N-SF57. The optical performance of the various prism set is simulated and analyzed by using optical ray tracing software, Zemax.

2.2 Schematic of relay lens system

To analyze the optical performance of the ATIR prism set in both of the paraxial system and the real system, different relay lens system is designed. The relay lens system consists of two relay lenses. The schematic of relay lens system is shown in Fig. 2 for the two prisms with BK7.

In Fig.2(a), paraxial relay system indicates the combination of ideal relay system and ATIR prism. When ideal relay system combines the TIR prism, the optical path is considered and kept at constant. In the paraxial relay system, the spot size variation at different regions and the corresponding lateral color aberration are only contributed by the ATIR prism owing the relay lens are aberration-free. The relation among the spot size, θ_{in} , prism material and region of DMD is shown in [13]. Nevertheless, the paraxial relay system is only for quickly evaluate the optical system and cannot be

realized in a practical projection system. The real relay lens system is needed to replace the paraxial relay system for fully evaluating the performance of the optical system. In the real relay system, the material of the relay lens is chosen to be poly-methyl 2-methylpropenoate (PMMA) for low cost.

2.3 ATIR prism in paraxial relay system

In the paraxial relay system, the lateral color aberration of illumination system is only determined by ATIR prism because the paraxial relay system ignores the chromatic aberration. The relation between the lateral color aberration, prism size, and θ_{in} in the paraxial relay lens system is shown in Fig.3. For different optical materials, the trend of the lateral color aberrations as a function of θ_{in} is similar. The angle as lateral color aberration goes to minimum is defined as θ_M . In addition, the hollow symbols represent the prism size as a function of θ_{in} . In order to obtain a compact prism size, the θ_{in} is limited within -20° to 20° [1]. For $-20^\circ < \theta_{in} < 20^\circ$, we are able to find θ_M , which means a solution of the achromatic prism set.

There is the minimum lateral color aberration at θ_M . Different optical materials result in different θ_M . In addition, when θ_{in} increases from θ_M , the lateral color aberration increases. Almost all materials follow this trend, except for N-SF57 in type2 prism set. On the other hand, θ_M is positive value for type1 while θ_M is negative value for type 2. With different materials, Abbe number affects the value of θ_M . It shows negative correlation between Abbe number and θ_M for the type1 prism set. On contrary, it shows positive correlation between Abbe number and θ_M for the type2 prism set.

2.4 ATIR prism in real relay system

In real relay system, the lateral color aberration is both contributed by real relay system and ATIR prism set. The lateral color aberration and the prism size as a function of θ_{in} for the real relay system is shown in Fig.4. As shown in Fig.4(a), θ_M exists at a specific θ_{in} which presents an achromatic condition. When Abbe number (V_1) decreases, θ_M becomes larger. The performance of lateral color aberration in the real relay system is similar to that of the paraxial relay system. Due to the effect of real relay system, N-LAF2 and N-SF2 have almost the same θ_M . Under the same θ_M , the prism size and n_1 are in negative correlation, as discussed in the previous section. Therefore, N-LAF2 has smaller prism size due to large n_1 . In type2 prism, the lateral color aberration and the prism size as a function of θ_{in} are shown in Fig.4(b). The solid symbols represent the lateral color aberrations as a function of θ_{in} . Similar to the result of the paraxial relay system, the θ_M of N-SF57 is located at $\theta_{in} < -20^\circ$. When the optical material with an Abbe number (V_2) is applied, it leads to a larger θ_M . The prism size decreases for a decreasing θ_M .

Here, we make a comparison of Fig.3 and 4. For the lateral color aberration issue, we obtain the similar

performance between paraxial and real relay system, such as the effect of Abbe number. Nevertheless, the θ_M of the paraxial relay system is different from that of the real relay system. When ATIR prism is analyzed in the real relay system, the lateral color aberration is also affected by the real relay system due to the dispersion nature of a real lens. In addition, there is similar phenomenon in type2 prism. For the prism size issue, the variation of prism size with different θ_{in} is almost the same in real and paraxial relay system because the architecture of prism will not be affected by the real relay system. Nevertheless, the prism size decreases because of an increasing θ_M . With the same material, the prism size in real relay system is smaller than that in paraxial relay system.

2.5 Angle loss and efficiency loss

Besides of the chromatic aberration, the efficiency is also considered. In order to rapidly evaluate the efficiency loss, a factor, angle loss, is defined as the rays which cannot pass through the surfaces and interfaces of prisms. The angle loss occurs when rays pass through the interface between the prisms and air gap. There are two positions where the angle loss might occur, i.e. surface1 and surface2, as shown in Fig.5. Therefore, we simply divide the angle loss into two parts: one is angle loss1 at the surface1, another is angle loss2 at the surface2

At the surface1, the angle loss1 exists when TIR happens at the upward marginal ray in illumination system. Here, the angle of the upward marginal ray at surface1 is denoted by θ_{LA1} and the angle of the first prism is denoted by θ_1 , respectively. In addition, the difference between θ_{LA1} and the critical angle at surface1 is defined as θ_{D1} . For $\theta_{D1} > 0$, θ_{LA1} is larger than the critical angle. Consequently, the angle loss1 occurs due to TIR effect. For a larger θ_{D1} , the angle loss1 increases. On contrary to the surface1, the surface2 is a reflective surface based on TIR effect. At surface2, the incident angles of rays reflected from the DMD chip smaller than the TIR angle lead to the angle loss2. Under the projection lens system, the chief ray, upward marginal ray and downward marginal ray are shown in Fig.1. The angle loss2 occurs at downward marginal ray in projection lens system. The angle of the downward marginal ray at surface2 is denoted by θ_{LA2} and the difference between θ_{LA2} and critical angle at surface2 is denoted by θ_{D2} , respectively. As $\theta_{D2} < 0$, it suffers from the angle loss 2. The angle loss2 increases for a smaller θ_{D2} .

In order to analyze the angle loss, the θ_{LA1} , θ_{LA2} and critical angle with different materials are discussed. The θ_{LA1} , θ_{LA2} , critical angle as a function of θ_{in} is shown in Figs.6 and 7. In order to prevent angle loss, θ_{LA1} is less and θ_{LA2} is greater than the critical angle. In order to analyze the relationship between angle loss and

efficiency loss, these designs are simulated using the commercial raytracing software, Lighttools. The efficiency loss can be divided into efficiency loss1 and efficiency loss2, respectively. The efficiency loss1 due to the angle loss 1. Table1(a) lists the efficiency type 1 prism set. Almost all rays arrive the surface 2 and the efficiency loss1 are less than 1%. Nevertheless, the efficiency loss2 is significant and the total efficiency decreases. Table1(b) lists the efficiency loss, θ_{D1} , θ_{D2} , θ_{LA1} , θ_{LA2} and critical angle for type2 prism set. When N-LAF2 and N-SF57 are applied as the materials of the second prism, there are significant efficiency loss1 due to large refractive index.

3. CONCLUSION

In this paper, two type ATIR prisms are designed and analyzed. For type1 prism, the lateral color aberration, prism size, cost and efficiency loss, are compared for five different materials. Thus, N-SF2 is chosen for the first prism. When θ_M is 14° , the lateral color aberration is $0.65 \mu\text{m}$ in the real relay system. The prism size is 2305 mm^3 . The efficiency loss is 15.05% due to angle loss. In type2 prism, the optical performance of five materials is also compared under the reasonable range of θ_{in} . Therefore, N-SSK8 is chosen as the second prism. When θ_M is -3° , the lateral color aberration is $0.61 \mu\text{m}$. The prism size is 3000 mm^3 . The efficiency loss is less than 1%. Based on the above result of two type ATIR prisms, their advantages and disadvantages are all analyzed and discussed. Type 1 prism performs a smaller prism size, lower cost but with a high efficiency loss. On the other hand, type2 prism performs a low efficiency loss.

Fig. 1. Schematic of the optical path of the ATIR prisms with different materials.

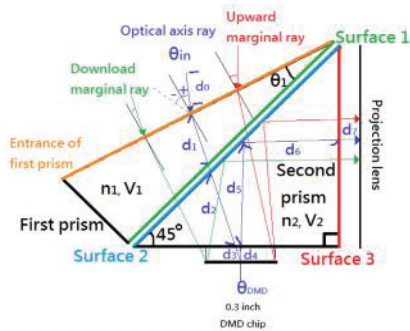


Fig. 2. Optical path of the investigated relay lens system. (a) Paraxial Relay System with the ATR prism. (b) Real Relay System.

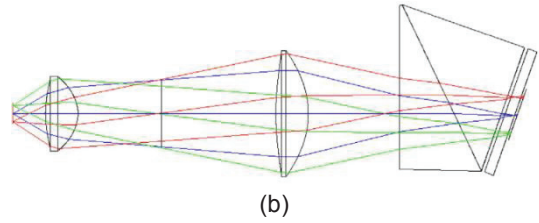
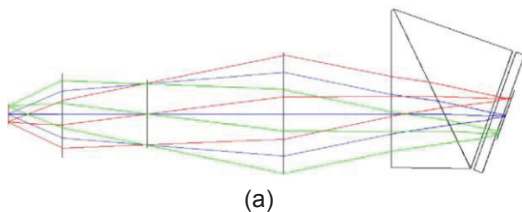


Fig. 3. Lateral color aberration and prism size as a function of θ_{in} in paraxial relay system. (a) Type 1 prism. (b) Type 2 prism.

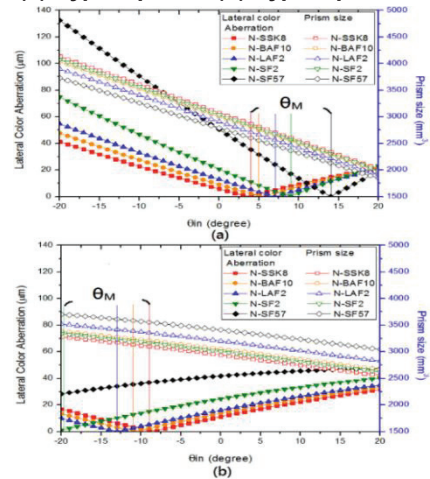


Fig.4. Lateral color aberration and prism size as a function of θ_{in} in the real relay system. (a) Type1 prism. (b) Type2 prism

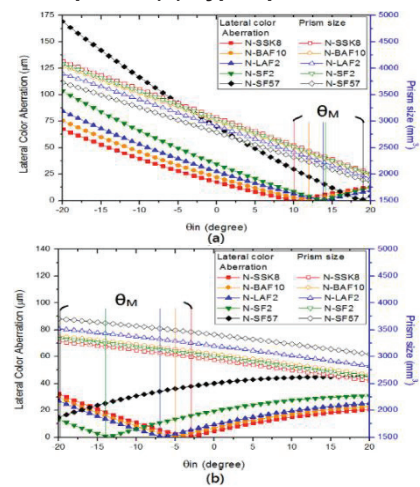


Fig. 5. Schematic of the incident angles at each surface of the ATIR prism.

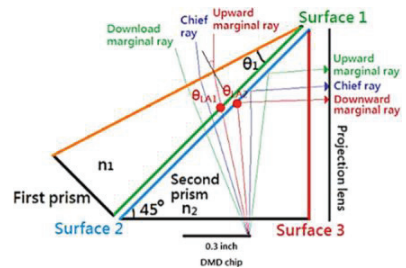


Fig.6. (a) θ_{LA1} , (b) θ_{LA2} , and critical angle as a function of θ_{in} for the type1 prism case.

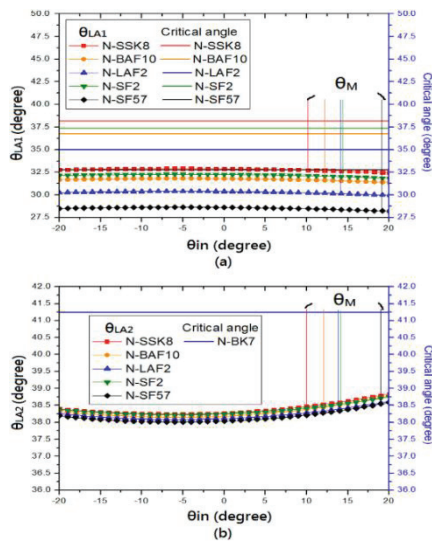


Fig.7. (a) θ_{LA1} , (b) θ_{LA2} , and critical angle as a function of θ_{in} for the type2 prism case.

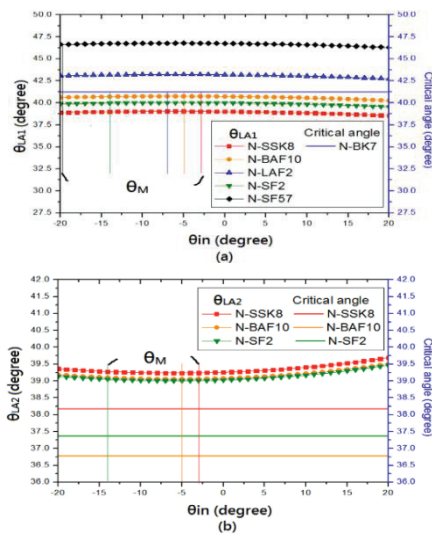


Table.1. The analysis of efficiency loss in (a) type1 (b) type2 prism

	N-SSK8	N-BAF10	N-LAF2	N-SF2	N-SF57
θ_{LA1} (degree)	33.28	32.10	30.61	32.51	28.65
Critical angle (degree)	38.18	36.78	34.99	37.37	32.79
θ_{D1} (degree)	-4.90	-4.68	-4.38	-4.86	-4.14
Efficiency loss 1 (%)	0	0	0	0	0
θ_{LA2} (degree)	38.47	38.45	38.40	38.53	38.54
Critical angle (degree)	41.25	41.25	41.25	41.25	41.25
θ_{D2} (degree)	-2.78	-2.80	-2.85	-2.72	-2.71
Efficiency loss 2 (%)	15.24	15.34	15.40	15.05	14.87

(a)

	N-SSK8	N-BAF10	N-LAF2	N-SF2	N-SF57
θ_{LA1} (degree)	39.04	40.75	43.22	39.98	46.64
Critical angle (degree)	41.25	41.25	41.25	41.25	41.25
θ_{D1} (degree)	-2.21	-0.50	1.97	-1.27	5.39
Efficiency loss 1 (%)	0	0	10.44	0	31.61
θ_{LA2} (degree)	39.24	39.06		39.05	
Critical angle (degree)	38.18	36.78		37.37	
θ_{D2} (degree)	1.05	2.28		1.68	
Efficiency loss 2 (%)	0.44	0.55		0.68	

(b)

REFERENCES

- [1] M.S. Brennesholtz, E.H. Stupp, Projection displays, in: Lasers as Projection Light Sources, (SID, 2008), pp. 180–190.
- [2] J.W. Pan, S.H. Tu, C.M. Wang, J.Y. Chang, High efficiency pocket-size projector with a compact projection lens and a light emitting diode-based light source system, Appl. Opt. 47 (19) (2008) 3406–3414.
- [3] M.Q. Liu, B.F. Rong, H.W.M. Salemin, Evaluation of LED application in general lighting, Opt. Eng. 46 (7) (2007) 074002.
- [4] E.F. Schubert, J.K. Kim, Solid-state light sources getting smart, Science 308 (5726) (2005) 1274–1278.
- [5] H.S. Murat, H.D. Smet, D. Cuypers, Compact LED projector with tapered light pipes for moderate light output applications, Displays 27 (3) (2006) 117–123
- [6] M. Huseyin, C. Dieter, D.S. Herbert, Design of new collection systems for multi LED light engines, Proc. SPIE 6196 (2006) 19604.
- [7] J.M. Teijido, F. Ludley, O. Ripoll, Compact three panel LED projector engine for portable applications, SID 37 (1) (2006) 2011–2014
- [8] Z. Tan, F. Zhang, T. Zhu, J. Xu, Bright and color-saturated emission from blue light-emitting diodes based on solution-processed colloidal nanocrystal quantum dots, Nano Lett. 7 (12) (2007) 3803–3807.
- [9] M. Huseyin, C. Dieter, D.S. Herbert, Design of new collection systems for multi LED light engines, Proc. SPIE 6196 (2006) 19604.
- [10] Texas Instruments (TI), DLP3000 DLP® 0.3 WVGA Series220DMD, <http://www.ticom/product/DLP3000>.
- [11] W.J. Smith, Modern optical engineering, in: The Achromatic Prism and the Direct Vision Prism, SPIE, 2008, pp. 126–128.
- [12] SCHOTT Glass Manufacturers, Optical Glass - Overview (Excel Table), <http://www.schott.com/>.
- [13] J.W. Pan, S.H. Lin, Achromatic design in the illumination system for a mini projector with LED light source, Opt. Express 19 (17) (2011) 15750–15759.